

## Cyclic testing of weak-axis steel moment connections

Kangmin Lee<sup>1</sup>, Rui Li<sup>\*1</sup>, Heetaek Jung<sup>2</sup>, Liuyi Chen<sup>1</sup> and Kyunghwan Oh<sup>3</sup>

<sup>1</sup> Department of Architectural Engineering, Chungnam National University, Daejeon, Korea

<sup>2</sup> 3D Engineering Co., Ltd., Seoul, Korea

<sup>3</sup> Engineering & Construction Group, Samsung C&T Corporation, Seoul, Korea

(Received March 18, 2013, Revised July 12, 2013, Accepted August 01, 2013)

**Abstract.** The seismic performance of six types of weak-axis steel moment connections was investigated through cyclic testing of six full-scale specimens. These weak-axis moment connections were the column-tree type, WUF-B type, FF-W type, WFP type, BFP-B type and DST type weak-axis connections. The testing results showed that each of these weak-axis connection types achieved excellent seismic performance, except the WFP and the WUF-B types. The WFP and WUF-B connections displayed poor seismic performance because a fracture appeared prematurely at the weld joint due to stress concentrations. The column-tree type connection showed the best seismic behavior such that the story drift ratio could reach 5%.

**Keywords:** moment resisting frame; weak-axis steel moment connection; cyclic testing; seismic performance; ductility

---

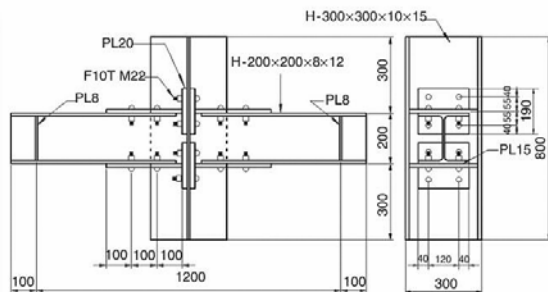
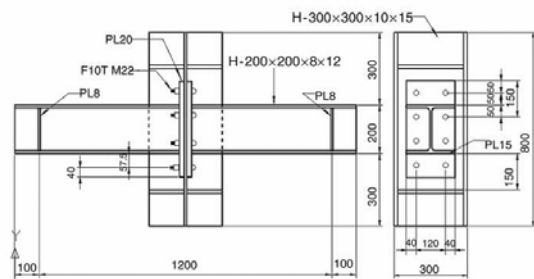
### 1. Introduction

Moment resisting frames (MRF) are widely used in steel structures as lateral force resisting systems due to their superior ductility and energy dissipation capacity. In 1994, a large earthquake centered in Northridge, California caused widespread damage to steel moment frame structures in the area. The majority of the damage occurred in the form of brittle fracture near the column-to-beam flange groove welds. Thus, the need to develop new connection details that have excellent seismic performance was highlighted. Prequalified connections were developed through research on the seismic performance of strong-axis connections (FEMA 2000) in the US. These post-Northridge strong-axis connections include reduced beam section connections and reinforced connections (Han *et al.* 2007, Girão Coelho and Bijlaard 2007). However, these studies mainly concentrated on strong-axis beam-to-column connections. It was difficult to find studies on weak-axis connections within Korea and other countries.

Kim *et al.* (2008) evaluated the structural performance of the split-tee type and end-plate type weak-axis connections, as shown in Figs. 1 and 2, respectively. For the split-tee weak-axis connection, the test results showed that the maximum resistance strength and ductility of the connection was improved with an increase in the number of shear connection bolts connecting the split tee connectors to the column web. Another guiding study was carried-out by Gilton and Uang

---

\*Corresponding author, Graduate Student, E-mail: class533@naver.com

Fig. 1 Split-tee type details (Kim *et al.* 2008)Fig. 2 End-plate type details (Kim *et al.* 2008)

(2002), in which a seismic performance of the reduced beam section (RBS) weak-axis connection was experimentally conducted. This study showed that the RBS weak-axis connection was able to reduce the strain concentration at the edge of the beam flange near the groove weld and achieved the required 0.03 radians of plastic rotation. These tests were conducted to provide a general indication of the possible performance of weak axis connections, however they are not considered to comprise a sufficient database for prequalification of such connections. Therefore, the seismic performance of weak-axis connections should definitely be evaluated through experimental research. In addition, through the comparisons of their seismic performances, some types of weak-axis connections showing excellent seismic performance would be adapted for steel moment frame connections.

For this purpose, an experimental program was designed and performed with six types of weak-axis steel moment connection details. These weak-axis moment connections were the column-tree type, the WUF-B type, the FF-W type, the WFP-W type, the BFP-B type, and the DST type weak-axis connections. These moment connection details have been used for strong-axis beam-to-column connections; in this study, these strong-axis prequalified connections were introduced as weak-axis connections. Each specimen was designed with the same beam and column sizes so that their seismic performance could be equitably compared.

## 2. Test program

In this research program, six full-scale weak-axis moment connections were tested using a predetermined cyclic deformation history. The six full-scale specimens were the column-tree (CT) type, welded unreinforced flanges, bolted web (WUF-B) type, bolted flange plate (BFP) type, welded flange plate (WFP) type, free flange (FF-W) type, and double split tee (DST) type specimens, respectively. The specimens were fabricated using H-shaped rolled steel. The beam size was H-600 × 200 × 11 × 17, and the column size was H-400 × 400 × 13 × 21. All beam and column section sizes of each specimen were the same to ensure that their seismic performance could be compared equitably. Generally, in order to prevent the soft-story damage, the strong column-weak beam system should be the structure system. The following relationship shall be satisfied at beam-column connections,  $\sum_{pc}^* M / \sum_{pb}^* M > 1.0$ , where  $\sum_{pc}^* M$  is the sum of the moments in the column above and below the joint at the intersection of the beam and column

centerline.  $\sum_{pb}^* M$  is the sum of the moments in the beam at the intersection of the beam and column centerline.

## 2.1 Test specimens

The specimen configurations are summarized in Table 1, and their details are shown in Fig. 3. These specimens offered a variety of connection types. These connection types are generally used for strong-axis beam-to-column connections. Except the column-tree type connection, the rest of the five types of connections were described in FEMA-350, as strong-axis prequalified connections. Column-tree type connections are in common use for moment frame structures in Korea and Japan. The column-tree connection is fabricated by welding stub beams to the column in the shop. Unlike the pre-Northridge connection case, the critical welding of the beam-to-column joint is performed in the shop, which can provide better quality control (Chen *et al.* 2006). The rest of the five specimens were manufactured according to prequalified connections defined in FEMA-350. The WUF-B specimen was fabricated in accordance with the pre-Northridge WUF-B beam-to-column connections. This type of connection is prequalified only for ordinary moment frame applications. The BFP connection utilizes flange plates welded to the column and bolted to the beam flange. This connection type induces several mechanisms of stable inelastic behaviour including panel zone distortion, bolt-slip, flange plate hinging, and girder hinging beyond the flange plate connection (Schneider and Teeraparbong 2002). The WFP specimen is similar to the BFP connection, but it is slightly different in that the flange plates were connected to the beam flanges by welding (Chen *et al.* 2007, Farrokhi *et al.* 2010). In the FF-W specimen, the web of the beam was removed in a single cut in the area adjacent to the column flange and was replaced with a heavy trapezoidal-shaped shear tab (Venti and Engelhardt 2000). The DST type connections are a type of partially restrained connection. This type of connection employs bolted split-tee connectors between the beam and the column web (Latour *et al.* 2011, Latour and Rizzano 2011).

In many practical cases, the panel zone strength has a great effect on the inelastic response of a moment connection. For strong-axis connections, the panel zone is a portion of the column web, but for weak-axis connections, the panel zone is a portion of the column flanges. Thus, in general, the panel zone strength of weak-axis connections is much higher than that of strong-axis connections. The panel zone strength ratio ( $V_y / V_{pzMy}$ ) of these weak-axis specimens was 2.35, where  $V_y$  is the panel zone yield strength and  $V_{pzMy}$  is the panel zone shear force when the connected beam yields.

Table 1 Weak-axis connection specimens

Specimen	Type	Applicative frame type	Fully/partially restrained	Flange joint	Web joint
CT	Column-tree	SMF	FR	Bolted	Bolted
WUF-B	Welded unreinforced flange-bolted web	OMF	FR	Welded	Bolted
BFP	Bolted flange plate	SMF	FR	Bolted	Bolted
WFP	Welded flange plate	SMF	FR	Welded	Welded
FF-W	Welded free flange	SMF	FR	Welded	Welded
DST	Double split tee	SMF	PR	Bolted	None

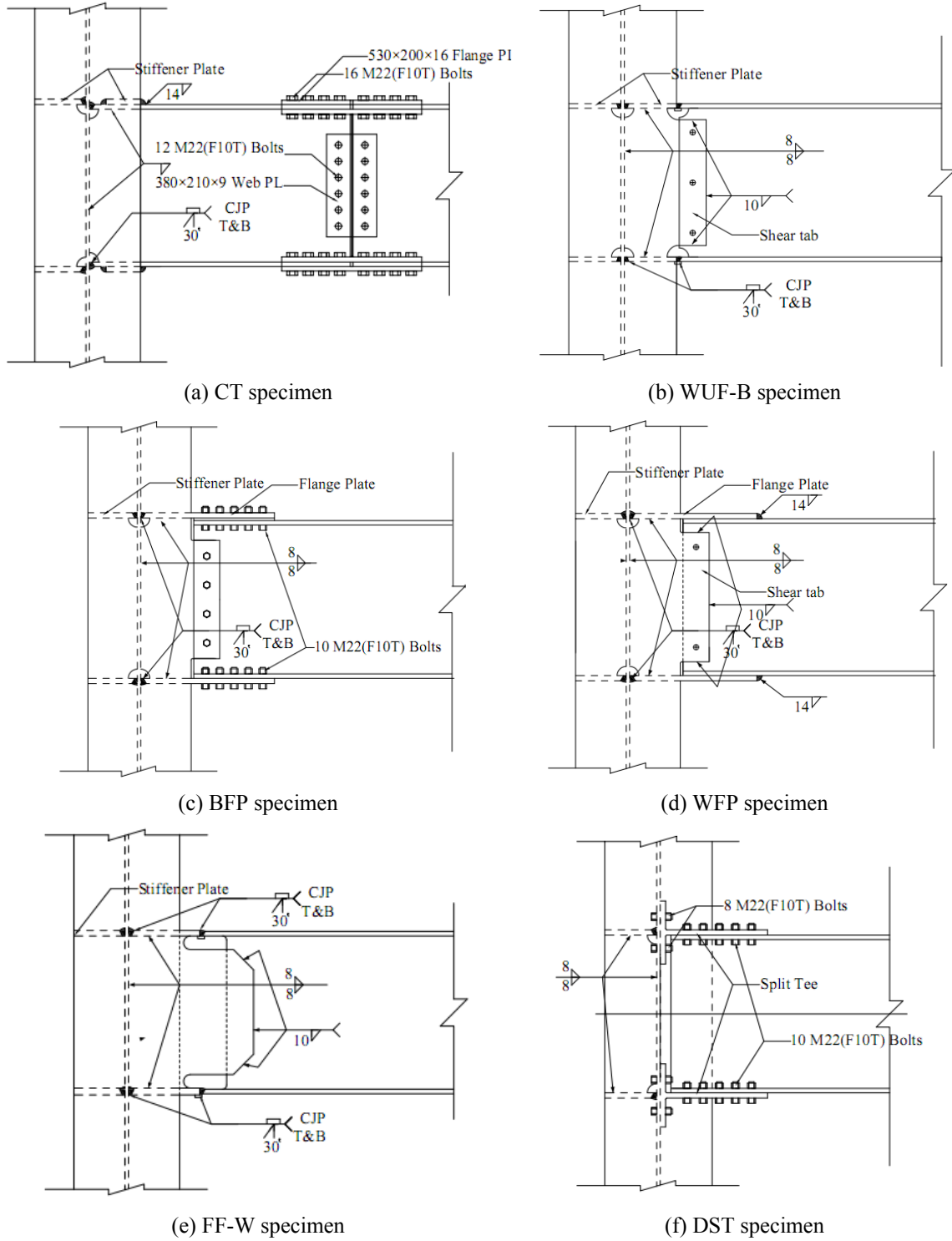


Fig. 3 Details of specimens

### 2.2 Test set-up and instrumentation

Each specimen was tested in the horizontal plane, as shown in Fig. 4. A 500 kN capacity actuator was used to impose the predetermined cyclic loads. Lateral supports were provided to prevent out of plane instability as well as twisting of the beam. Testing was conducted by controlling the level of axial or rotational deformation imposed on the specimens. Testing was stopped promptly when a specimen fractured, the maximum allowable deformation of the actuator was reached, or when the measured strength of the specimen dropped to 80% of the maximum strength. The test specimens were subjected to cyclic loads according to the requirements prescribed in Section S6.2 for beam-to-column connections of Seismic Provisions for Structural Steel Buildings (AISC 2010). The loading sequence is shown in Fig. 5.

Linear varying displacement transducers (LVDTs) were attached to the specimens to measure the displacement of structures. Also, strain gauges were attached to either sides of the beam web as well as the top and bottom of the beam flange to measure local strains. The layout of the LVDTs and the arrangement of strain gages are shown in Figs. 6 and 7. Before testing, specimens were whitewashed to observe the yielding of the components during the tests.

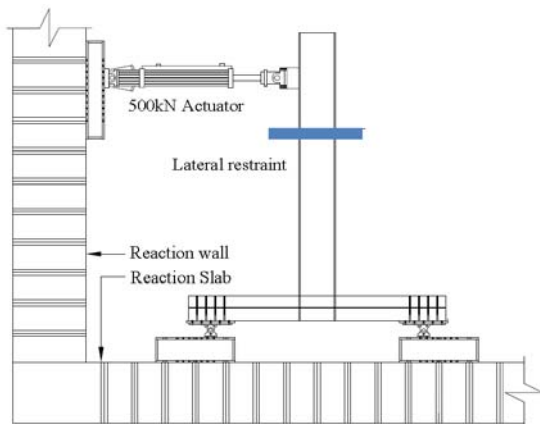


Fig. 4 Test setup

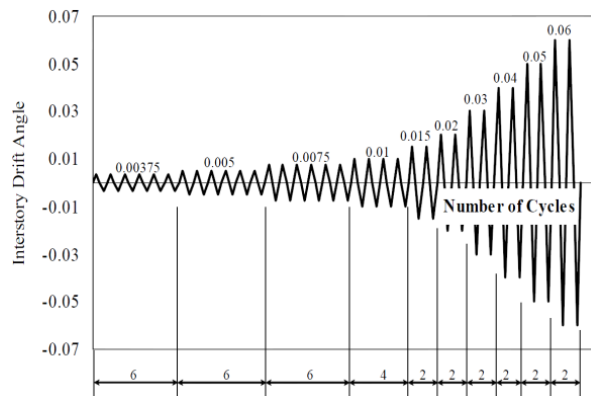


Fig. 5 Loading sequence

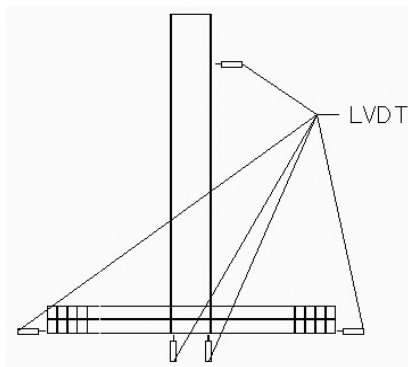


Fig. 6 LVDT layout

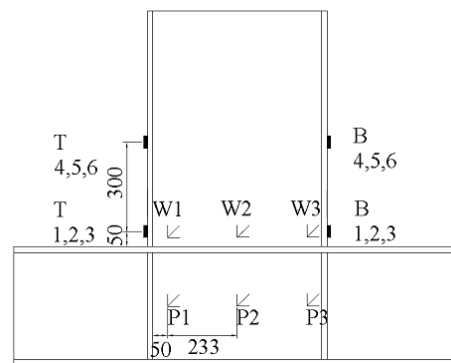


Fig. 7 Strain gage layout

### 3. Test results

#### 3.1 Material properties

Twelve coupons were collected respectively from the beam and column of the specimens. Then, each of these coupons was tested for mechanical properties. The test results are summarized in Table 2. Note that the actual yield strength of each coupon exceeded the nominal yield strength more than 1.2 times.

#### 3.2 Hysteretic curves

The story drift ratio plot for each of these specimens is shown in Fig. 8. These plots show behavior relative to a normalized moment, which is the total imposed moment divided by the plastic moment of the beam. Both total and plastic moments were computed with respect to the column flange face. The total moment  $M_f$  was obtained from the actuator loads times the distance of the actuators to the column flange face. The plastic moment  $M_p$  was computed using the actual material strength and cross-sectional properties of the beam.  $M_f/M_p$  is greater than 1 because of the overstrength resulting from the strain hardening of the connection components.

Table 2 Properties of the coupons

Shape	Location	Class	Actual yield / Nominal yield strength (MPa)	Tensile strength (MPa)	Yield ratio
H-400 × 400 × 13 × 12	Web	SM490	398.4/325	559.7	0.71
	Flange	SM490	407.9/315	571.4	0.71
H-600 × 200 × 13 × 12	Web	SS400	336.3/245	470.5	0.71
	Flange	SS400	292.3/235	455.8	0.64

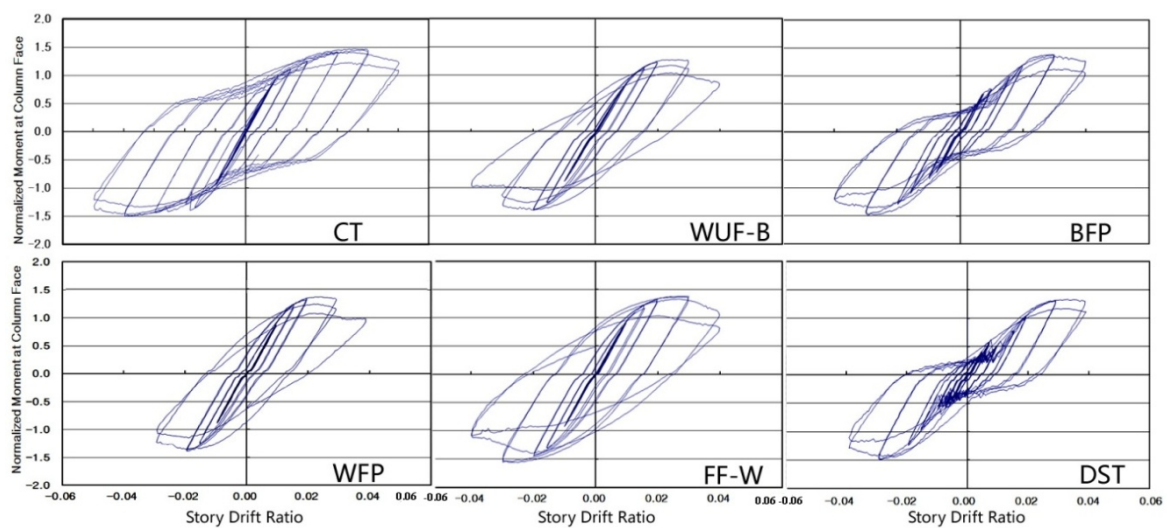


Fig. 8 Story drift ratio of specimens

As seen in Fig. 8, the CT, BFP and DST specimens showed excellent plastic rotation capacities because the bolted flange plate connection can absorb a significant amount of inelastic energy due to the slip of bolts. The other three specimens showed a similar variation tendency which was an apparent degradation of strength after the maximum resistance strength. Except the FF specimen, the WUF-B specimen and the WFP specimen showed poor plastic rotation capacities because an early fracture appeared at the weld joint. In the FF specimen, its web of the beam is removed in a single cut in the area adjacent to the column flange, and it is replaced with a heavy trapezoidal-shaped shear tab. Thus, free portions of the beam flanges significantly reduce the connection deformation constraints and allow the flange steel to yield freely. The local buckling of the free portions of the beam flanges can absorb a significant amount of inelastic energy.

In general, the cyclic behavior of each specimen can reflect the energy dissipation capacity of connections. As seen in Fig. 8, it can be estimated that the column-tree specimen had excellent seismic behavior, and the WUF-B and the WFP specimens showed relatively poor seismic behavior.

Also, note that the hysteretic curves of the CT, BFP and DST specimens have a pinched shape near origin. The reason for this phenomenon is that the beam flange joints of the CT, BFP and DST specimens were bolted connections, and those of the WUF-B, WFP and FF-W specimens were welded connections. Meanwhile, the slipping of bolts at about the normalized moment of 0.5 was observed from the hysteretic curves of the CT, BFP and DST specimens.

### 3.3 Mode of failure

The following discusses the observed behavior and the test results for each specimen.

#### 3.3.1 CT specimen

Failure of this specimen, as seen in Fig. 9(a), was local buckling of the beam flanges. Slipping of bolts was noticed during the cycles of 2% story drift ratio, while the gap of the beam splice unsymmetrically expanded. The local buckling of the beam top flange occurred during the cycles of 4% story drift ratio. Meanwhile, the gap of the beam splice slightly decreased. Finally, local buckling occurred at the beam top flange during the cycles of 5% story drift ratio. The resistance strength began to fall and the test was stopped at the maximum resistance strength of 80%.

#### 3.3.2 WUF-B specimen

Failure of this specimen, as seen in Fig. 9(b), was the fracture of the weld joint at the beam top flange. The yielding of the beam bottom flange was detected during the 1.5% cycles of story drift ratio. The yielding of the beam top flange occurred during the cycles of 2% story drift ratio. The maximum resistance strength was reached at 3% story drift ratio. When the fracture of the weld joint at the beam top flange expanded, the resistance strength rapidly decreased during the cycles of 4% story drift ratio.

#### 3.3.3 BFP specimen

Slipping between the flange plate and the beam below the flange occurred during the cycles of 2% story drift ratio, and this was caused by slipping of the bolts connecting the flange plates to the beam flanges. During the cycles of 3% story drift ratio, the yielding of the beams top flange occurred, and slipping between the beam web and the shear tab was detected. The maximum resistance strength appeared at 3% story drift ratio. Shear failure of the bolts connecting the flange plates to the beam flanges occurred at 4% story drift ratio as shown in Fig. 9(c). Eventually, the

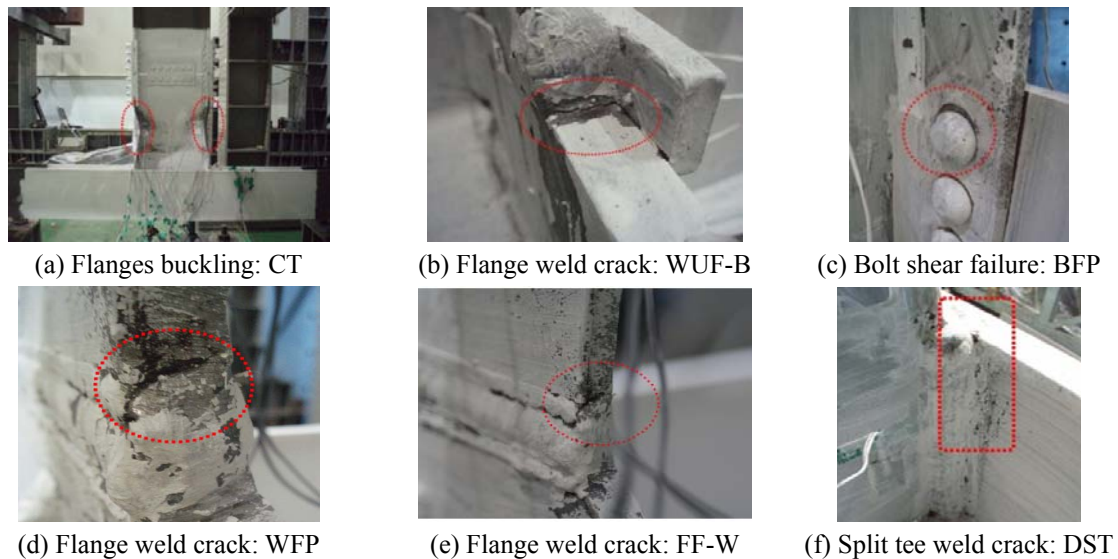


Fig. 9 Failure modes

resistance strength began to fall.

### 3.3.4 WFP specimen

The yielding of the beam top flange was detected during the cycles of 1.5% story drift ratio. During the cycles of 2% story drift ratio, local yielding took place at the beam web, and small cracks appeared at the weld joint connecting the top flange plate to the column. The maximum resistance strength was reached at 3% story drift ratio. Fracture occurred at the weld joint connecting the bottom beam flange to the flange plate as shown in Fig 9(d), and the bearing capacity reduced rapidly during the cycles of 4% story drift ratio.

### 3.3.5 FF-W specimen

The local buckling of the beam bottom flange occurred during 2% story drift ratio. Then, during the cycles of 3% story drift ratio, the local buckling of the beam top flange was detected. After that, fracture occurred at both the bottom and top beam flange welding zones, as shown in Fig. 9(e), and the resistance strength began to fall rapidly. The maximum resistance strength was detected at 3% story drift ratio. The resistance strength began to fall, and the test was stopped at 80% of maximum resistance strength.

### 3.3.6 DST specimen

Slipping between the below split-tee connector and the beam below flange occurred during the cycles of 1% story drift ratio. During the cycles of 2% story drift ratio, yielding of the split-tee connectors occurred. During the cycles of 3% story drift ratio, yielding of the beam flanges was detected. Then, yielding of the column panel zone appeared, and the weld joint between the split-tee connectors and the column flange was fractured, as shown in Fig. 9(f). Finally, the resistance strength began to fall, and the test was stopped at 80% of the maximum resistance strength.

Table 3 Experimental results

Specimen	$P_u$ (kN)	$\Delta_y$ (mm)	$\delta_i$ (%)	$\theta_p$ (rad)	Final failure mode
CT	277.5	188.1	4.96	0.038	Local buckling of beam flange
WUF-B	258.1	150.5	2.97	0.020	Fracture of beam flange welding
BFP	275.5	151.0	3.99	0.030	Bolts shear failure
WFP	285.1	150.3	2.92	0.019	Fracture of beam flange welding
FF-W	288.2	150.6	3.96	0.032	Fracture of beam flange welding
DST	271.2	151.4	3.79	0.028	Fracture of split-tee connectors welding

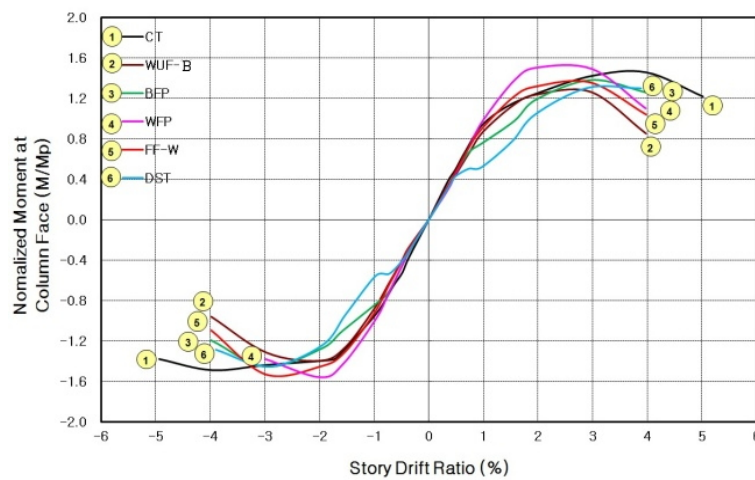


Fig. 10 Comparison of story drift ratio

Table 3 shows the maximum resistance strength, the maximum displacement  $\Delta_y$ , the story drift ratio  $\delta_i$ , the plastic rotation  $\theta_p$ , and final failure mode of specimens.

#### 4. Analysis of test result and investigation

##### 4.1 Seismic performance evaluation

According to the requirement of Seismic Provisions for Structural Steel Buildings (AISC 2010) approved by the AISC, for beam-to-column connections used in special moment frames (SMF), intermediate moment frames (IMF) and ordinary moment frames (OMF) shall be capable of sustaining a story drift ratio of at least 0.04, 0.03, and 0.01 radians, respectively. Also, the moment strength of the beam-to-column connection must be able to sustain more than 80% of the beam nominal plastic moment strength.

The story drift ratio curves are compared in Fig. 10; thus, it is possible to compare the seismic performance of the six specimens. In this test, the CT specimen showed the best seismic performance such that the maximum story drift ratio reached 0.05 radians, and the moment strength was more than 80% the nominal plastic moment strength. The WUF-B specimen showed

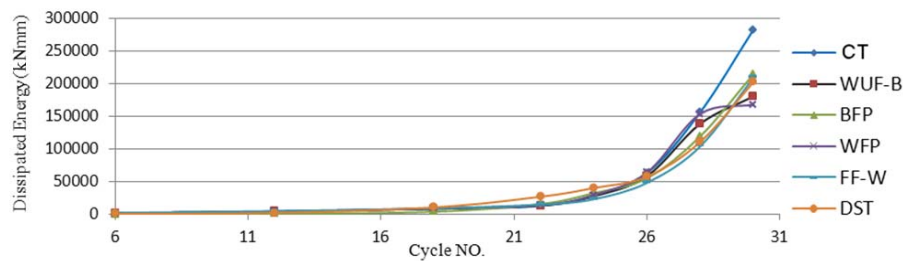


Fig. 11 Comparison of dissipated energy

poor seismic performance because the degradation of strength was serious. This can be attributed to the fracture in the weld joint at the beam flanges. In the WFP specimen a brittle fracture appeared unexpectedly; therefore, the story drift ratio only reached 0.03 radians. The BFP, FF-W, and DST specimens achieved the similar seismic performance; they could sustain a story drift ratio of 0.04 radians, and the moment strength was more than 80% the nominal plastic moment strength.

#### 4.2 Energy dissipation capacity

The energy dissipation capacity is an important index to evaluate the seismic performance of beam-to-column moment connections, and it can be reflected through the area of the load-displacement hysteretic loop. The bigger the area of a hysteretic loop is, the better the dissipation capacity is. Fig. 11 shows a comparison of cumulative energy dissipation with increasing cycles. As seen in Fig. 11, the CT specimen had the best energy dissipation capacity, and the connections whose beam flanges were connected by bolts were slightly better than the connections which were beam flange welded connections. For the FF-W specimen, the local buckling of free portions of beam flanges dissipated a lot of inelastic energy; thus, its energy dissipation capacity was better than that of the WUF-B and WFP specimens.

## 5. Conclusions

A total of six specimens, including the CT, WUF-B, FF-W, WFP-W, BFP and DST type weak-axis moment connections respectively, were tested cyclically to investigate their seismic performance. The following conclusions can be made from the experimental study:

- For the CT type connection, local buckling of the beam flange appeared at a story drift ratio of 0.05 radians. Then, the resistance strength of the specimen began to slowly fall. According to the experimental results, its story drift ratio reached 0.05 radians, and it had the biggest energy dissipation capacity. This means that the CT type specimen had the best seismic performance among these six specimens.
- For the WUF-B specimen, as a type of pre-Northridge connections, the fracture of the beam flange weld joint occurred at the story drift ratio of 0.03 radians. Then, the resistance strength of the specimen began to fall rapidly.
- In the BFP specimen, shear failure of the bolts connecting the flange plates to the beam flanges appeared at a story drift ratio of 0.04. It satisfied the requirement of reaching the story drift ratio of 0.04. However, a very important point to note is that the slip

characteristics at the joint of the flange plates and the beam flange that caused the bolts to slip should be researched through further experiment and analysis.

- For the WFP connection, a fracture appeared prematurely at the weld joint connecting the top flange plate to the column due to stress concentrations during the cycles of 2% story drift ratio. The story drift ratio only reached 0.03 radians. The WFP specimen, which is a type of prequalified connection prescribed in FEMA-350, should have a good seismic performance as originally intended, but brittle failure occurred. The reasons for premature fracture need further research in the future.
- The FF-W specimen showed excellent seismic performance. The total plastic rotation achieved 0.03 rad, and its energy dissipation capacity was also excellent and may be attributed to the local buckling of the free portions of the beam flanges.
- The DST specimen also showed excellent seismic performance. The moment strength of the specimen could still sustain more than the beam nominal plastic moment strength of 80% when the story drift ratio reached 0.04 rad.

## Acknowledgements

This research was supported by Basic Science Research Program through the National Research Foundation of Korea (NRF) funded by the Ministry of Education, Science and Technology (grant number: 2012R1A1A4A01004350).

## References

- AISC (2010), *Seismic Provision for Structural Steel Building*, American Institute of Steel Structure, Chicago, IL, USA.
- Chen, C.C., Lin, C.C. and Lin, C.H. (2006), "Ductile moment connections used in steel column-tree moment-resisting frames", *J. Constr. Steel Res.*, **62**(8), 793-801.
- Chen, J., Su, M., Shen L., Cai, Y. and Guo, H. (2007), "Experimental study on steel moment resistant frame connections with welded flange plates", *J. Build. Struct.*, **2007**(3), 1-7.
- Farrokh, T., Danesh, F.A. and Eshghi, S. (2010), "The structural detailing effect on seismic behavior of steel moment resisting connections", *Struct. Eng. Mech., Int. J.*, **35**(5), 617-630
- FEMA (2000), "Recommended Seismic Design Criteria for New Steel Moment-Frame Buildings: FEMA-350", SAC Joint Venture, Richmond, Caliph, USA.
- Gilton, C.S. and Uang, C.-M. (2002), "Cyclic response and design recommendations of weak-axis reduced beam section moment connections", *J. Struct. Eng. ASCE*, **128**(4), 452-463.
- Girão Coelho, A.M. and Bijlaard, F.S.K. (2007), "Experimental behavior of high strength steel end-plate connections", *J. Constr. Steel Res.*, **63**(9), 1228-1240.
- Han, S.W., Kwon, G.U. and Moon, K.H. (2007), "Cyclic behaviour of post-Northridge WUF-B connections", *J. Constr. Steel Res.*, **63**(3), 365-374.
- Kim, S.D., Kim, S.S. and Ju, Y.K. (2008), "Strength evaluation of beam-column connection in the weak axis of H-shaped column", *Eng. Struct.*, **30**(6), 1699-1710.
- Latour, M. and Rizzano, G. (2011), "Experimental behavior and mechanical modeling of dissipative t-stub connections", *J. Struct. Eng.*, **138**(2), 170-182.
- Latour, M., Piluso, V. and Rizzano, G. (2011), "Experimental analysis of innovative dissipative bolted double split tee beam-to-column connections", *Steel Construct.*, **4**(2), 53-64.
- Schneider, S.P. and Teeraparbong, I. (2002), "Inelastic behavior of bolted flange plate connections", *J. Struct. Eng.*, **128**(4), 492-500.

Venti, M. and Engelhardt, M.D. (2000), “Test of a free flange connection with a composite floor slab”, *SAC Background Document SAC/BD-00/18*, SAC Joint Venture, Richmond, CA, USA.

CC